ASME Journal of Tribology
Online journal at:
https://asmedigitalcollection.asme.org/tribology

Nick Morris[1]
Wolfson School of Mechanical, Electrical and Manufacturing Engineering, Loughborough University, Leicestershire LE11 3TU, UK
e-mail: n.j.morris@lboro.ac.uk

Ramin Rahmani
Wolfson School of Mechanical, Electrical and Manufacturing Engineering, Loughborough University, Leicestershire LE11 3TU, UK
e-mail: r.rahmani@lboro.ac.uk

Homer Rahnejat
Wolfson School of Mechanical, Electrical and Manufacturing Engineering, Loughborough University, Leicestershire LE11 3TU, UK;
School of Engineering, University of Central Lancashire, Preston, Lancashire PR1 2HE, UK
e-mail: hrahnejat@uclan.ac.uk

Bharat Bhushan
Department of Mechanical and Aerospace Engineering, The Ohio State University, San Jose, CA 95120
e-mail: bhushan100@outlook.com

Air Foil Thrust and Journal Bearing Coatings: A Review

Surfaces of air foil thrust and journal bearings in high-speed turbomachinery are coated to improve their operational integrity, particularly when the aerodynamic load-carrying capacity is reduced during instances of startup and shutdown. Surface coatings, as protective barriers in air foil bearings, can mitigate the adverse effects of direct surface interactions on such occasions. This article provides an in-depth review of the body of important research conducted for the study of coated air foil thrust and journal bearings, highlighting the state of the art in coating technology. The review features the role of composite coatings, designed to provide favorable thermal, mechanical, and frictional characteristics. This article also highlights the trends in the selection of coatings for air foil bearings, pertinent to desired thermo-mechanical performance. [DOI: 10.1115/1.4065986]

Keywords: air foil bearings, surface coatings, turbomachinery, thrust bearings, journal bearings, bearing design and technology, gas (air) bearings

1 Introduction

Air foil thrust and journal bearings are used in a variety of high-speed turbomachinery applications, such as in cryogenic turbo-expanders, turbochargers, high-temperature blowers, micro-power generation gas turbines, and aircraft air cycling machines [1]. The bearing design provides for an oil-free, high-speed low-friction axial and radial load support during the operation of turbo-compressors and expanders. Oil-free bearing system design is critically important in applications such as hydrogen compression, where contaminants should be kept to a minimum.

Air foil bearings operate through entrainment of air into a thin converging gap created between the foil and a thrust runner or journal. The fluid-structure elasto-aerodynamic interactions of the entrained air and thin flexible foil create a lubricating film of air, separating the contiguous surfaces. Air foil journal bearings can support loads of up to approximately 10 kN radially and operate at speeds upwards of 150,000 rpm. Axial loads and speeds for foil thrust bearings are shown in Fig. 1. During startup and shutdown operations, the entrainment speed is quite low and the generated hydrodynamic (aerodynamic) load-carrying capacity is insufficient to fully separate the contiguous surfaces, resulting in their direct contact. The surfaces of the foil and the thrust runner may also come into direct contact during destabilizing impact events or because of external excitations. To protect against such instances, surface coatings are employed to enhance the foil, the journal, and runner's durability, robustness, and frictional behavior.

A number of relatively recent reviews have documented the development and the state-of-the-art in air foil-bearing design [1–4]. Despite numerous advantages, foil, journal, and thrust bearings have comparatively low load-carrying capacities compared with their liquid phase counterparts. As already noted, air foil bearings suffer direct surface contact during startup and shutdown. Therefore, surface coatings are critical in preventing premature wear of top foil journal and top foil runner interfaces [5,6]. The key properties of coatings, substrates, and coating—substrate combinations for air bearings are described by Bhushan et al. [7] as

- good mechanical properties: ductility, hardness, and yield strength
- dimensional stability
- corrosion and oxidation resistance
- contiguous surface coating comparability
- thermal and mechanical shock resistance
- thermal conductivity to transfer heat from the interface
- formation of soft protective oxide films
- low surface friction and wear
- good antigalling property if the coating is penetrated
- substrate-coating compatibility

[1]Corresponding author.

Contributed by the Tribology Division of ASME for publication in the Journal of Tribology. Manuscript received March 21, 2024; final manuscript received July 5, 2024; published online September 9, 2024. Assoc. Editor: Robert Fleming.

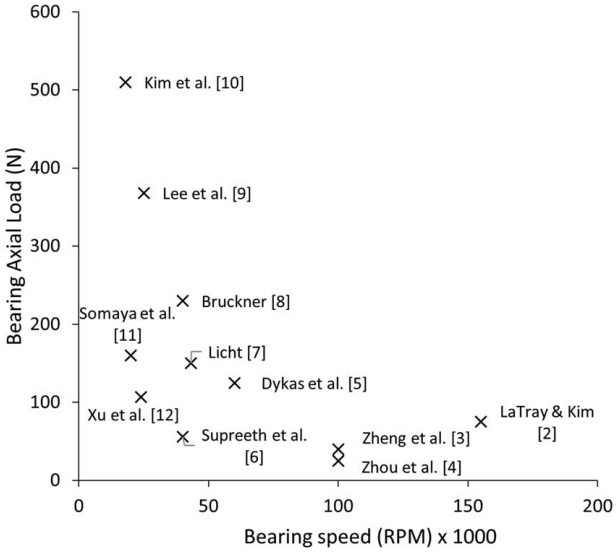

Fig. 1 Foil thrust bearing load-carrying capacity and upper operating speed

- thermal properties comparable between coating, adhesion layer, and substrate

This paper reviews the application of specific thermo-mechanical conditions at the interface of air foil bearings' sliding surfaces. The state-of-the-art in air foil thrust and journal bearings' coating technologies is highlighted. Trends in coating design are identified and the direction for future air foil-bearing coatings is discussed.

2 Physics of Air Foil-Bearing Coating

2.1 Hydrodynamic Regime of Lubrication. The entrainment of air into the converging wedge geometry formed by the top foil and the stator endows the bearing with a hydrodynamic load-carrying capacity. However, at high dynamic loads, experienced below the bearing lift-off speed, the film of air is usually insufficient to fully separate the contiguous surfaces. The Stribeck fluid film ratio, also known as the lambda ratio (λ), is an indicator of the likelihood of direct contact of surfaces. It is defined as

$$\lambda = \frac{h}{\sqrt{\sigma_1^2 + \sigma_2^2}} \tag{1}$$

where λ is the lubricant film ratio parameter and σ_1 and σ_2 are the root mean square surface roughness of the runner and foil surfaces, respectively. The value of λ>4 indicates the full separation of contacting surfaces. However, during startup or shutdown operations, the film thickness, h, may reduce as there is a diminution of air entrainment. This decreases the hydrodynamic load-carrying capacity, promoting the onset of mixed or even boundary regimes of lubrication.

The surface coating in journal and thrust foil bearings has been shown to affect the transition from full film hydrodynamic regime to mixed and boundary regimes of lubrication [8–11]. One mechanism for this is the interfacial slip caused by the breakdown of the continuum mechanics behavior of the gas. The prevalence of this behavior is described by the nominal Knudsen number [12,13] as

$$\mathrm{Kn} = \frac{k_b T}{\sqrt{2}\pi\delta^2 p h_m} \tag{2}$$

where k_b is the Boltzmann constant, δ is the kinetic molecular diameter, p is the static pressure, and T is temperature. For Kngt0.01, then the magnitude of slip is regarded as significant [13,14], and the fluid should be treated as a rarefied gas. Lee et al. [14] have shown that at 1000 K the Knudsen number can be 0.16 for gas foil bearings.

2.2 Thermal Effects. Foil bearings are often required to operate in environments with elevated temperatures due to the nature of their application, for example in micro-gas turbines. Additionally, the air film temperature increases as a result of parasitic viscous shear and compressive heating during entrainment [15]. The primary mechanism of heat transfer within the air film is conduction across the film thickness [16]. Convective heat transfer is limited due to the low density of air. Lehn [16] showed that for air foil thrust bearings approximately 80% of the heat is dissipated away from the contact through convective heat transfer from the reverse side of the rotor disc and through the top foil-to-bump foil and base plates (Fig. 2). Secondary cooling effects include radial convective heat transfer to the housing and forced convection via the air supplied through the bump foils. Salehi et al. [17] also showed similar results for air foil journal bearings, where 80% of the heat transfer took place by conduction through the journal and foils. The remaining 20% was transferred through side leakage.

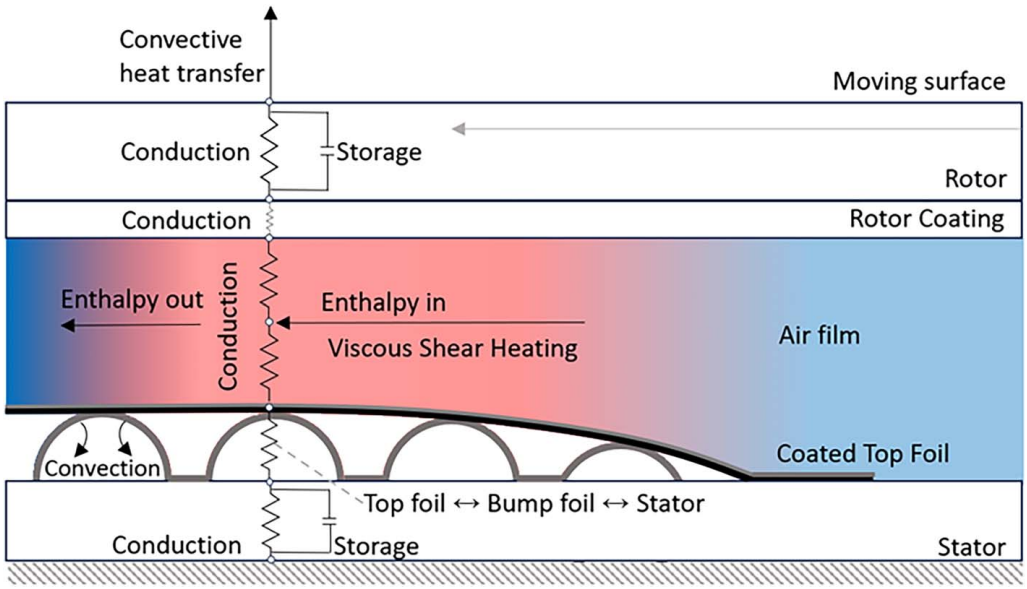

Fig. 2 Primary heat transfer paths of an air bearing in full film hydrodynamic regime of lubrication

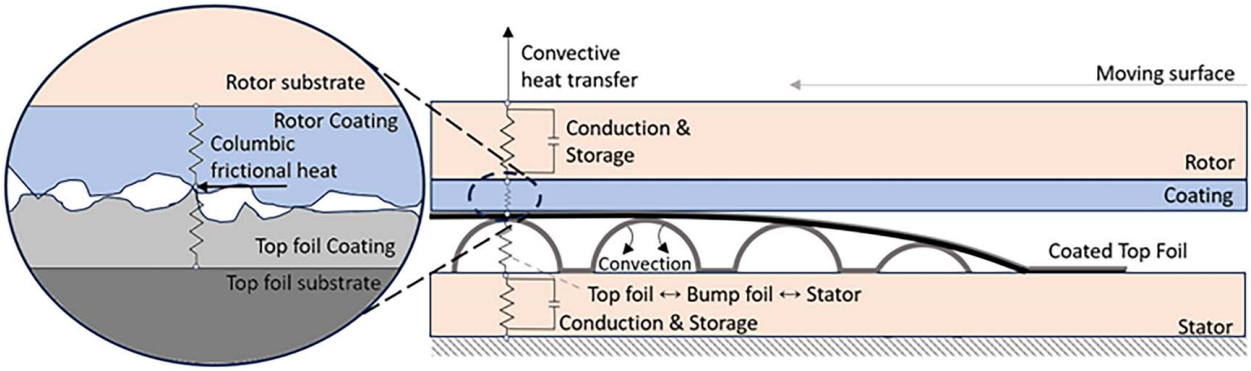

Fig. 3 Primary heat transfer paths in an air bearing under boundary regime of lubrication

During machine startup and shutdown direct contact of the top foil and rotor leads to the generation of coulombic frictional heating. On these occasions, machine performance becomes most critical and challenging in nature. The following thermal analysis considers the interfacial thermal problem in the absence of a mediating film of air and in the first instance considers the contacting solid bodies as semiinfinite.

The coated thrust runner and journal both move relative to the frictional heat source, created at their interface with the foil. During the transient heat transfer process, the penetration depth of the heat flow into the coating can be determined as [18]

$$D = \frac{L}{\sqrt{1+Pe}}, \text{ for Pe} = \omega R_e L/4\kappa_{1c} > 0.1 \tag{3}$$

where Pe is the Peclet number, representing the ratio of heat advection rate to the rate of diffusion, ω is the angular velocity, R_e is the effective contact radius, L is the length of the square-shaped frictional contact area, and κ_{1c} is the thermal diffusivity of the journal or rotor coating. Typically, the heat penetration depth, D, is less than or comparable to the coating thickness for most appreciable speeds. Therefore, the thermal properties of the coating are of particular importance for the determination of interfacial temperature. As a result, the thermal properties of the journal and rotor coating are considered when apportioning the generated frictional heat between the contiguous surfaces as described by Kennedy and Tian [19]:

$$\gamma = \frac{q_2}{q} = \frac{1}{1+\dfrac{K_{1c}}{K_{2s}}\sqrt{1+Pe}} \tag{4}$$

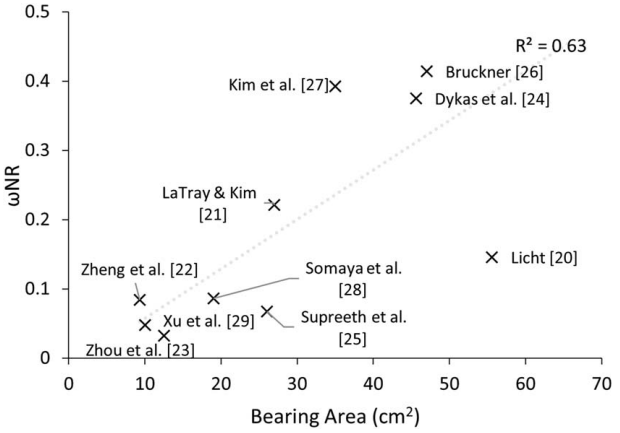

Fig. 4 The product of rotational speed, load, and radius from the generated heat by coulombic friction (Eq. (5)) against bearing area

where γ is the heat partitioning factor, K_{1c} and K_{2s} are the thermal conductivities of the rotor or journal coating, and the foil substrate, respectively, and q and q_2 are the total generated frictional heat and that transferred to the foil, respectively. As a result, in both full film and boundary regimes of lubrication thermal conductivity of the surfaces remain critical to the determination of air film and interfacial temperatures as shown in Figs. 2 and 3. The coating's thermal conductivity and thickness alongside the contact area should be considered so as not to introduce additional thermal barriers. The generated heat rate between the two bodies in boundary regime lubrication due to coulombic friction is [12,19]

$$\dot{q} = \mu N R_e \omega \tag{5}$$

where N is the carried load and μ is the coefficient of friction. While the friction coefficient μ is difficult to characterize, the other parameters in Eq. (5) are readily available in the open literature. These parameters are plotted against the bearing area in Fig. 4. A clear relationship is shown between frictional heat dissipation and the designed bearing area.

The ratio of flash temperature rise, with and without a coating, for the case Pegt10 can be described as [18]

$$\tau = \frac{K_{1s}}{K_{1c}}\sqrt{\frac{\kappa_{1s}}{\kappa_{1c}}}, \text{ for Pe} > 10 \tag{6}$$

It can be seen that the thermal conductivity and diffusivity of the coating material should be greater than that of the exposed substrate for a reduction in interfacial flash temperature. The maximum contact surface temperature rise can be determined as [30]

$$T_m = \frac{2L\dot{q}}{\sqrt{\pi}\left(K_{2s} + K_{1c}\sqrt{1+Pe}\right)} \tag{7}$$

Thrust runners experience radially increasing velocities, often leading to a convex runner surface as a result of viscous heat dissipation and thermal expansion. In addition, centrifugal stress distortions in the runner can occur. To account for these distortions, structural tailoring and compliant foundations are used which are key for effective coating performance [31].

In addition to bearing thermal management, thermally induced failure modes associated with surface coatings should be considered. For example, thermal interfacial stress gradients between the coating and the substrate should be minimized. The change in stress due to thermal gradient can be calculated as shown by Holmberg and Matthews [32]:

$$\Delta\sigma_T = (\alpha_s - \alpha_c)\Delta T \frac{E_c}{1-\nu_c} \tag{8}$$

where α_s is the substrate's coefficient of thermal expansion, α_c is that of the coating's, and E_c and v_c are the Young's modulus of elasticity and Poisson's ratio of the coating. ΔT is the temperature difference between the center of the coating and the substrate. A simple thermal analysis to ascertain the mean coating temperature difference with the substrate yields

$$\Delta T = \frac{1}{2}\gamma\omega T_f \frac{d}{AK_{2c}} \tag{9}$$

where T_f is the frictional torque, d is the thickness of the coating, A is the frictional area, and K_{2c} is the thermal conductivity of the foil coating. Through matching coating and substrate thermal expansion coefficients, and introducing intermediary layers (if necessary), the additional stress component can be minimized [33].

2.3 Coating Contact Mechanics. Coating–substrate adhesion is critical for preventing delamination of the coating at their interface [34]. The propensity for delamination and spalling is dependent on the interfacial fracture energy and varies with substrate and coating elasticity, hardness, and ductility [32,34]. With specific regard to the foil coatings, the flexural strength of the coating is the key attribute for its adhesive performance.

The selection of coating pairs with complementary hardness is important to ensure effective running-in and long-term performance of the bearing. The importance of hardness compatibility in the foil-bearing coating system selection is shown in Fig. 5. The results shown in Fig. 5 are taken from an investigation of a foil journal bearing with various coatings [35]. When the foil coating is harder than the journal coating (positive abscissa values), the journal roughness reduces during operation. However, these tests were rated as unsuccessful, in the majority of cases, due to significant reported foil coating wear. In the cases when the much softer coatings are used on the foil, the journal roughness is largely unaffected and all the successful tests are found in this region (within the thermal limits of the coating). Other combinations were also tested in Ref. [35]; however, the hardness data were not available.

With direct contact with contiguous surfaces, abrasive and adhesive wear may occur. Adhesive wear occurs at the atomic scale contact of contiguous surfaces, at locations with high asperity contact pressure, leading to plastic deformation of the asperities and shakedown. The plasticity index, defined by Greenwood and Williamson [36] comprises the ratio E'/H which is known to be an important parameter in minimizing plastic wear during boundary friction:

$$\Psi = \frac{E'}{H}\sqrt{\frac{\sigma}{\beta}} \tag{10}$$

where Ψ is the plasticity index, E' is the reduced elastic modulus of the contact, H is the hardness, σ is the root mean square roughness, and β is the average tip radius of curvature of asperities. Clearly, the plasticity index can be reduced by changing the material properties ratio E'/H or surface topography characteristics σ/β. The junction adhesion can be suppressed by formed surface tribofilms. However, under persistent sliding, these films can be removed and contact between nascent surfaces occurs. In addition, careful selection of material-coupled crystalline structures and chemistry can avoid the usual problem of solid solubility for the contact with similar material surfaces. For ductile metals, Archard and Hirst [37] showed that the abrasive wear volume can be predicted from

$$W = K\frac{N}{H} \tag{11}$$

where K is the wear coefficient, N is the normal force, and H is the surface hardness. Hornbogen [38] and Bhushan and Gupta [39] showed that, for brittle materials, fracture toughness should also be considered when evaluating the wear volume, using [40]

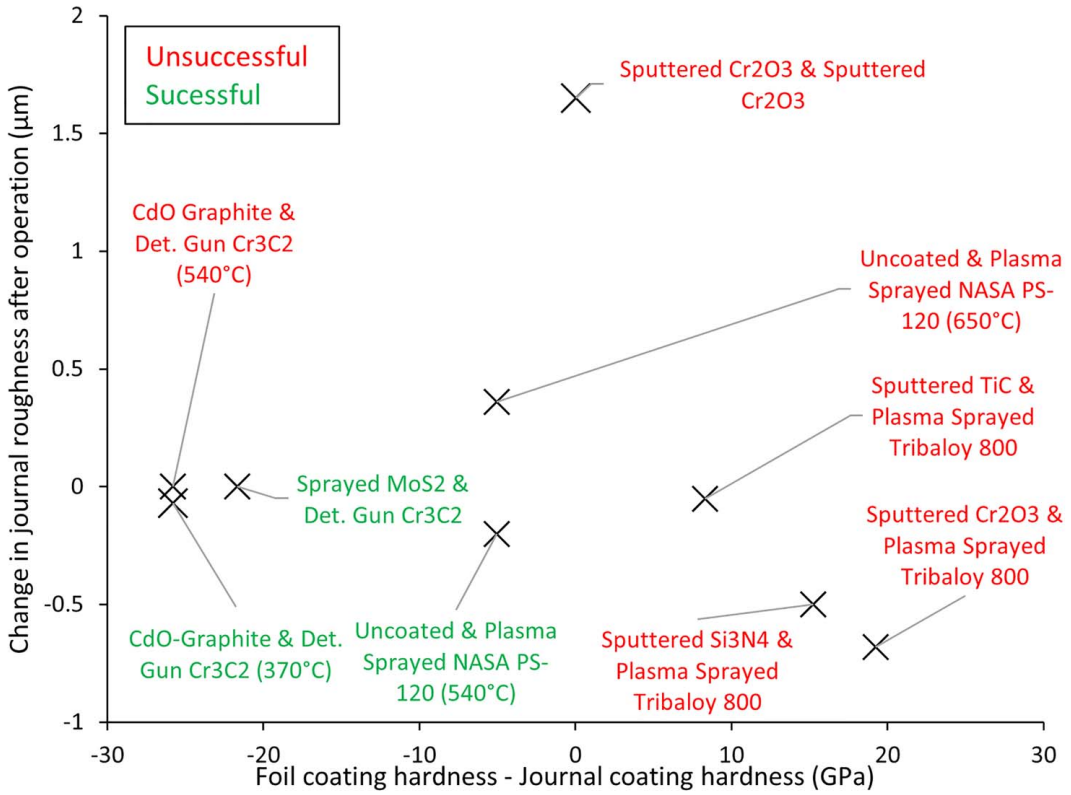

Fig. 5 Change in surface roughness between new and used surfaces against the difference in foil and journal coating hardness. Data are reported by Bhushan and Gray [35].

$$W = ck_o \frac{\sigma_y m^2 E' p^{3/2}}{K_{IC}^2 H^{3/2}} \quad (12)$$

where c is an empirically determined constant, k_o is the wear coefficient, σ_y is yield stress, m is work hardening exponent, K_{Ic} is the plane strain fracture toughness, and E' is the composite elastic modulus.

The ratio E'/H in Eq. (10) and a variant of it in Eq. (12) relate to the coating and substrate system to accumulate elastic strain before failure and is the key parameter in determining tribological performance and elastic resilience of the interface in an impact [41].

The flexural strength of the coating is also of importance due to contact deformation of the top foil and thermo-mechanical distortion of the thrust rotor. It has been shown that multilayer coatings, comprising inter-layers of low elastic moduli reduce the bending stresses in comparison to the hard coatings alone [41]. In addition, the use of thin hard coatings is effective at reducing bending stress and improving fatigue life [42].

Much more attention should be paid to the failure of coatings, often caused by generated sub-surface stresses as the result of combined direct normal loading and shear [43,44]. However, most contact mechanics analyses are developed for nonconforming contacts, mainly based on Hertzian or neo-Hertzian conditions, where the contacting surfaces may be considered semiinfinite in nature. This is not usually the case for thin hard coatings, regarded as thin bonded layered solids with various degrees of conformity [45,46]. Solutions for coated surfaces of hard materials with various degrees of conformity now exist, opening the way for detailed contact mechanics analysis of air foil and journal bearings.

In summary, a variety of thermo-mechanical coating—substrate and coating—coating properties have been identified so far. These properties will be used later for the critical review of the current state-of-the-art air foil-bearing coatings.

2.4 Coating Deposition Techniques. A variety of coating techniques are available for foil, journal, and thrust runner surfaces. Before the coating is applied, the substrate condition may determine the appropriate method for surface preparation. For example, the use of undercoats may be necessary to prevent the oxidation of ferrous substrates, and surface cleaning procedures or surface roughening.

A variety of techniques are prevalent for foil coating. These include physical vapor deposition (PVD) techniques such as sputtering [47,38], radio frequency (RF) plasma-assisted chemical vapor deposition [8], electroplating [8], fusion process [49], and other proprietary processes [6]. Thermal spray processes, including the use of a detonation gun, high-velocity oxygen fuel spray, plasma spray, and flame spray are considered too aggressive for thin foil substrates. Plasma spray coatings may require surface roughening pretreatments, such as grit blasting which have been shown to adversely damage the foil [6]. Although detonation gun coating does not usually require any pretreatment, foils tend to wrinkle and distort due to mechanical and thermal stresses even when continuously cooled [6].

A key element of the method of coating is the bonding strength, and the coating's ability to handle high centrifugal and thermal stresses. For example, PS304 HVOF with small nickel-chromium (Ni-Cr) and Cr_2O_3 particle sizes have been used to reduce PS304 coating roughness after finishing with polishing papers and compounds. Although initial roughening during operation provides little benefit in terms of roughness characteristics [50], improvements in bond strength in comparison to plasma spray methods have been noted. For thick (~100 μm) hard face coatings by plasma and detonation gun methods, further efforts have been made to improve PS304 dimensional stability through heat treatment cycles [51]. Composition grading to reduce the generated thermal stresses is also proposed in Ref. [51]. Alternatively, electroplating can produce thinner (~1-μm-thin dense chromium coatings). Reduced coating thickness lowers stresses due to centrifugal and thermal sources [50].

3 A Review of Journal Foil-Bearing Coatings

Broadly three categories may be used for applications of coatings in foil bearings: (i) low-temperature applications <300 °C, (ii) mid-range temperature applications: 300–700 °C, and (iii) high-temperature applications >700 °C. The journal substrate material is typically air-hardened AISI A2 tool steel [52], or A-286 age-hardened, or iron-nickel-chromium superalloy or similar materials [53]. Foil substrates are commonly made of nickel-based superalloys such as Inconel X-750, Inconel 625, or Inconel 718. They are primarily chosen for their high-temperature mechanical properties.

3.1 Low-Temperature Applications (<300 °C). Polyimide, polyamide, and polytetrafluoroethylene (PTFE) foil coatings are generally limited to a maximum temperature of 250 °C and are frequently paired with a hard chromium or thin dense chromium-coated surface. This action produces favorable antigalling characteristics in case the polymer foil coating is worn through. These coated films are often doped with a solid lubricant such as graphite, molybdenum disulfide (MoS_2), and boron nitride. Polymer coatings provide low cost and acceptable life performance when not subjected to excessive temperatures [54]. Zywica et al. [5,55] showed that a commercially available fluoropolymeric coating (AS20) paired with a Cr_2O_3-coated journal could present an acceptable wear behavior for 10,000 start–stop cycles at room temperature with minimal wear. The maximum operating temperature of the coating was given as 280 °C.

3.2 Mid-Range Temperature Applications (300–700 °C). WS_2 and MoS_2 overlays have been shown to provide promising results by Bagiński and Żywica [56], who used a foil-bearing test rig with a chromium oxide Cr_2O_3-coated journal to show that MoS_2 provided the lowest friction. However, the MoS_2/C (carbon-doped molybdenum disulfide) on a hard titanium aluminum nitride (TiAlN) provided the best trade-off between friction and wear, notably outperforming a WS_2 overlay. A comparison of the coatings is highlighted in Fig. 6. Critically, all the experiments were conducted at cold startup conditions and therefore, the results do not indicate high-temperature performance. Interestingly, WS_2 and the carbon-doped MoS_2/C are reported to have the same maximum operating temperature of 500 °C [39,56].

Korolon™ developed by Mohawk Innovative Technology Inc has been used in ramjet and gas turbine engines. Tungsten disulfide WS_2 (Korolon™ 900 and Korolon™ 800) overlays have been shown to be highly effective for both friction and wear performance [8,9,57]. WS_2 top foil coatings have been shown to perform well against chromium-coated journals [8,9,57]. Furthermore, Heshmat et al. [57] showed excellent wear and friction behavior for dense chromium-coated journals against WS_2 with a sacrificial solid lubricant overcoat (Korolon™ 800). A comparison of coating performance under initial testing at 650 °C is shown in Fig. 7. The coating was demonstrated on a 240-lb thrust turbojet engine, conducting 70 stop–start cycles (up to 54,000 rpm) over a running period of 14 h.

Bhushan and Gray [58] investigated the thermal stability of a number of candidate foil and journal coatings using extended duration tests (300 h) and thermal cycling up to temperatures of 650 °C. It was shown that sputtered foil coatings of TiC, Cr_2O_3, and Si_3N_4 and CdO-graphite and chemically adherent chromium oxide were statically thermally stable. In the case of the journal: plasma-sprayed Ni-Cr-bonded CrB_2, Co-Mo-Cr-Si with Ni-aluminide undercoat, Cr_3C_2 with Ni-Cr binder and NASA PS106 (Ni-Cr-Ag-CaF_2) alongside sputtered Cr_2O_3 and chemically adherent chrome-oxide had most promising static thermal stability. Bhushan [59,60] optimized and characterized RF sputtering parameters for depositing hard refractory chromium oxide coating onto Inconel X-750 foils. Bhushan [61] developed and tested a CdO-graphite-Ag coating using extended start–stop air foil journal bearing tests at temperatures up to 427 °C and 14 kPa

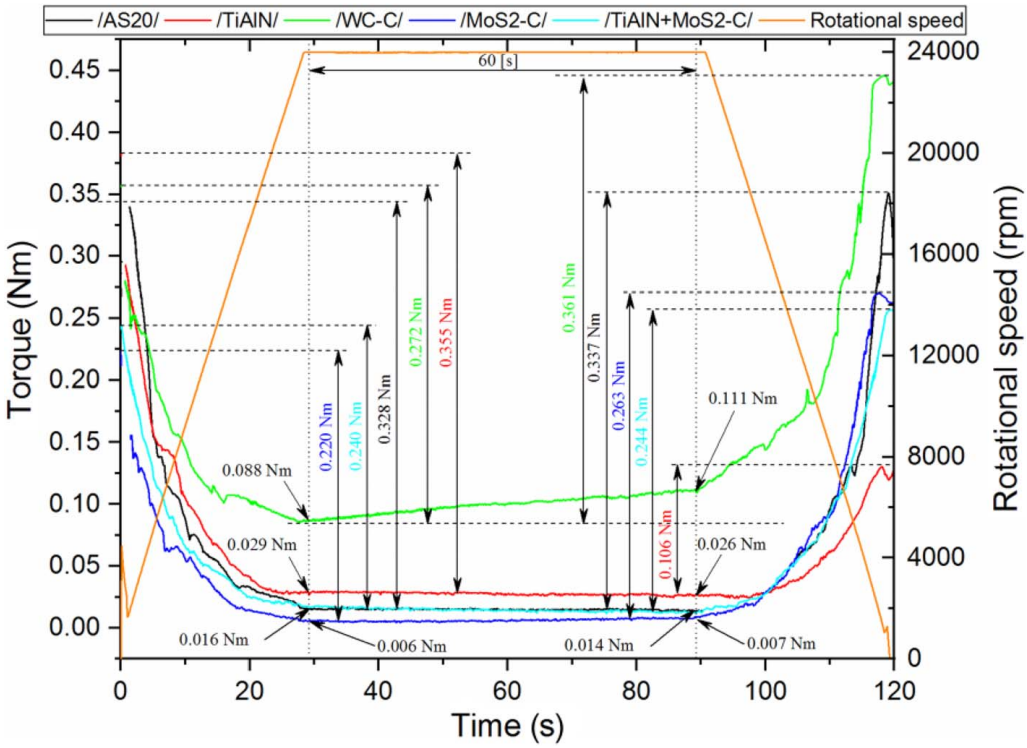

Fig. 6 A graph of torque variation in time for the last measurement cycles of the loaded bearing with different coatings. Reproduced with permission from Ref. [56].

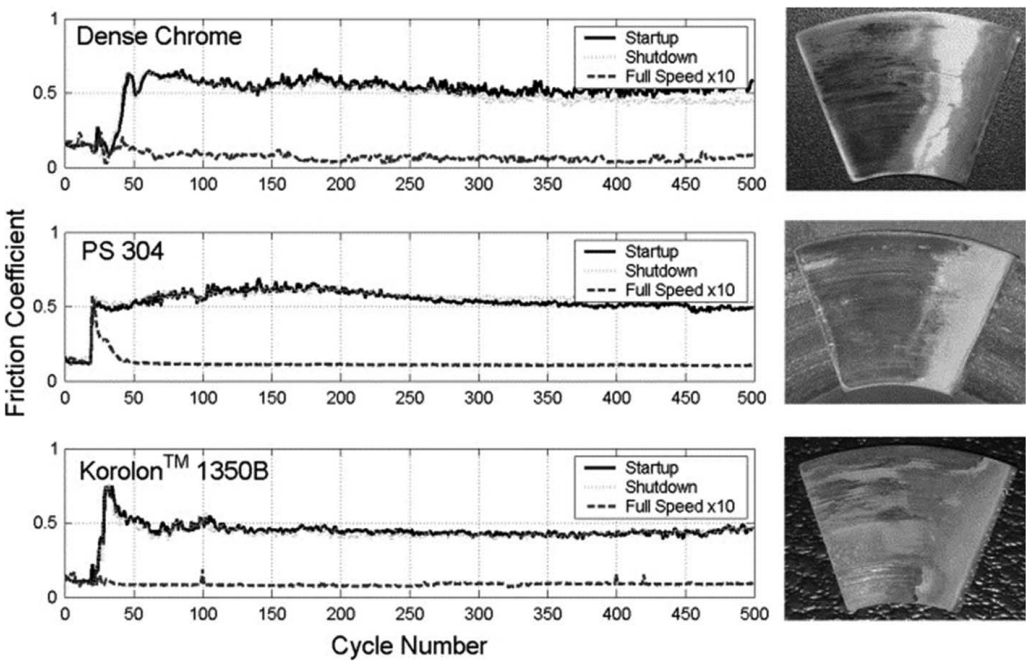

Fig. 7 Startup, shutdown, and full-speed friction coefficients for the composite coating C/B tested at 650 °C against three disk coatings; and posttest pad appearance. Reproduced with permission from Ref. [57]. Copyright 2005 by Elsevier.

contact pressure. The coating endurance was improved by introducing ultrafine silver, performing 9000 start–stop cycles at 288 °C and 28 kPa and 3000 cycles at 35 kPa.

In an exhaustive experimental study, Bhushan and Gray [35] investigated 15 combinations of foil and journal coatings using a bearing test rig. The most promising combinations for <370 °C were a foil coated with CdO and graphite and a chrome carbide-coated journal. While for temperatures <540 °C, a foil coated with NASA PS-120 (Tribaloy 400, silver, and CaF_2) against an uncoated foil, and for temperatures <650 °C, both the foil and

journal should be coated by a chemically adherent Cr_2O_3. The chemically adherent Cr_2O_3 coating system was successfully tested with a load of 35 kPa for 2000 start–stop cycles. Bhushan [53] showed that chromium oxide coating, sputtered onto an InconelX-750 foil, running against a detonation gun applied chromium carbide on an A286 journal performed very well during a variety of start–stop, impact, and static oven tests. The coating successfully completed 3000 cycles at a temperature of 650 °C and was subjected to a normal pressure of 14 kPa in a partial arc bearing test. This included 9000 start–stop cycles at a maximum test temperature of 427 °C, although the coating could have continued for much longer under these conditions. During start–stop cycles at a higher pressure of 35 kPa the coatings survived for 3000 start–stop cycles. The coatings also survived 100 g impact accelerations with the journal running at 30,000 rpm. The roughness of contiguous surfaces was 0.05 μm and the coating thickness was ~1 μm.

Chromium oxide (Cr_2O_3) was used in the work of Zywica et al. [5], covering a steel journal using a plasma-spraying technique. For this application, the bearing foil was made of Inconel Alloy 625. A thin polymer coating (AS20) was also applied on one side of the top foil to prevent any damage to the foil during startup and shutdown. The coating was chosen for reduction of friction, based on experimental work investigating a range of commercially available coatings including (AS18, AS20, AS48, AS783, and AS785) and composite and nanocomposites such as MoS_2TiW and nc-Wc/a-C. They also highlighted the importance of shortening the duration of startup/shutdown phases, noting that polymer coatings produced a rapid temperature rise during the running-in period which subsequently decreased. Bhushan [53] found that Cr_2O_3 was effective as a foil coating.

The use of vanadium nitride (VN) and TiSiN (applied to both front and back surfaces of the foil) and MoS_2 on the front surface in gas foil bearings was investigated by San Andrés and Jung [62] under a pressure of 25.6 kPa at 50,000 rpm with applied excitation frequencies in the range of 200–400 Hz. The use of VN and TiSiN-coated top foils was shown to reduce the energy losses during startup and shutdown. However, all tests were conducted at room temperature.

3.3 High Temperature (>700 °C). For high temperatures, Bhushan [63] developed a coating combining hard-wearing Cr_2O_3 and the ductility and thermal expansion coefficient of a nickel chromium combination (Ni 80%: Cr 20%) binder. The coating was applied to journal foils and compared with a sputtered Cr_2O_3 coating using start–stop and high-speed rubbing tests. A chrome carbide-coated journal surface was used for both. The $C_{r2}O_3$ completed the test (9000 cycles) while the Cr_2O_3 with Ni-Cr completed 3000 cycles. Interestingly the Cr_2O_3 with metallic binder had significantly lower friction at 650 °C compared with room temperature [43]. Later PS304, a composite solid lubricant coating, was developed. The coating comprised silver (10% wt), eutectic barium fluoride (BaF_2) (5% wt), and calcium fluoride (CaF_2) (5% wt), combined with chromium oxide (Cr_2O_3) as a hardener (20% wt) within a Ni-Cr matrix, acting as a binder (60% wt) [64]. The roughness of the coating is dependent on the deposition and finishing technique used. Using HVOF instead of plasma spray and small particle sizes and 1500 grit SiC paper for polishing, roughness values of 0.05 μm can be achieved. PS304 acts as a solid lubricant coating originally developed to address the limitations of chromium carbide coating in terms of reliability and high processing costs [50]. In addition, PS304 has been shown to initially roughen during running-in before polishing to a desirable roughness of <0.1 μm [50]. PS400 improved the performance by reducing the need for postprocessing to achieve an acceptable surface finish. DellaCorte and Edmonds [65] showed high temperatures (e.g., 800 °C) are required initially to create a lubricious glaze. After the glaze was formed during an initial high-temperature run, the low-temperature frictional performance was much improved. Heshmat et al. [50] concluded that directly applied thin dense chrome on the foil and run against the same, or alternative high-temperature coating on the shaft, provides an excellent life at temperatures of up to 820 °C in comparison to PS304. Stanford and DellaCorte [66] used a novel ion diffusion technique to apply CU-4Al coatings to foils. They tested the coating against a PS304-coated journal using a bearing test rig. The experiments indicated the foil coating assisted with break in and gave more stable friction across a range of temperatures and reduced top foil wear.

4 A Review of Foil Thrust Bearing Coatings

As with the case of journal bearings, the review of thrust air foil bearings is divided into low-temperature, mid-range temperature, and high-temperature applications. The thrust runner is typically steel, while the foils (like in the case of foil journal bearings) are commonly made of Inconel X-750, Inconel 625, or Inconel 718.

4.1 Low-Temperature Applications (<300 °C). Kim et al. [67] showed the effective use of a PTFE thrust bearing-coated top foil. However, they did not mention the runner material or its coating. Balducchi et al. [68] also used a PTFE-coated top foil against a hard-coated titanium runner. Walker et al. [69] investigated a wide range of foil coatings using a scratch test machine to investigate their cohesive and adhesive behavior as well as thermal stability using a high-temperature oven. The investigated PTFE coating was not favored for further testing. However, Ni-P and Si-O (13–23 μm), MoS_2, WS_2, and PS400 were recommended. Interestingly, MoS_2 showed a wide standard deviation for measured roughness values after heating when compared with WS_2. WS_2 is known to have a higher maximum operating temperature, reported as 500 °C [18], although some have reported even higher values [60]. An organically bonded (Dow-Corning Molykote 88) MoS_2-coated thrust air-bearing top foil and a flame-plated Cr_2O_3-coated runner were shown to provide acceptable performance during adverse operating conditions [61].

4.2. Mid-Range Temperature Applications (300–700 °C). Heshmat et al. [57] compared a variety of Korolon™ coatings on an Inconel X-750 top foil, including a polymer-based coating containing solid lubricants. A WS_2 coating with solid lubricants and a nickel chromium coating (also containing solid lubricants) (Korolon™ 1350A) with and without a WS_2 overcoat (Korolon™ 800) have also been investigated. These combinations were paired with a variety of coatings on the journal surface, including a PS304 plasma-sprayed hard chromium coating. Heshmat et al. [57] used a thrust bearing pad tribometer for a series of ramp-up and shutdown tests at 30–810 °C for 100- to 500-s cycles. They found a dense chromium coating against a WS_2 with a solid lubricant overcoat of a nickel-chrome provides the best tribological performance. The maximum service temperature of the WS_2 with a solid lubricant overcoat is 385 °C and for the case of nickel-chromium coating is 800 °C. The coating was demonstrated on a 240-lb thrust turbojet engine, conducting 70 start–stop cycles (up to 54,000 rpm) over a running period of 14 h. Jahanmir et al. [8,9] conducted room temperature tests for WS_2 coating (Korolon™ 900) against counter-faces of DLC, chromium, or hydrogenated DLC. It was found that at room temperature the performance of the DLC and chromium surfaces were quite similar. At high temperature (500 °C), the H-DLC provided the lowest coefficient of friction in the boundary regime of lubrication. However, reduced hydrodynamic lift at high temperature was noted. The DLC coating was found to induce a higher wear-rate on the pad coating. The increase in WS_2 wear with DLC was attributed to its hardness but also PEVD DLC films have been shown to have high nanoscale roughness [70,71] (see Eqs. (10) and (11)). For all surfaces, the benefits were observed when the WS_2 film was on the foil and the hard coating was applied to the runner.

4.3 High Temperature (>700 °C). Fanning and Blanchet [10] investigated coatings for air foil thrust bearings using a test rig

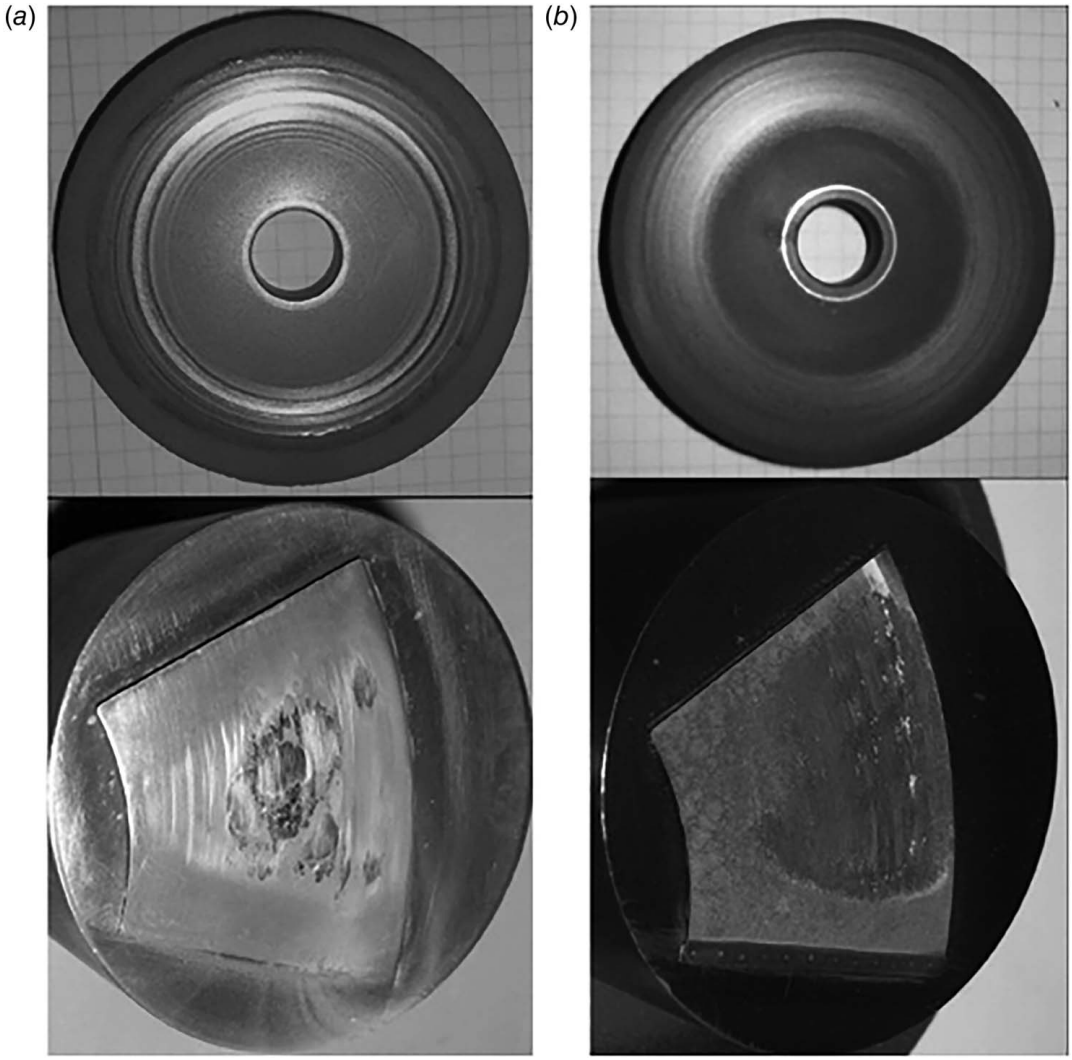

Fig. 8 Worn disk and pad surfaces from tests with PS304-coated (plasma-sprayed) disks against (*a*) uncoated and (*b*) K1350A-coated pad. Reproduced with permission from Ref. [10]. Copyright 2008 by Elsevier.

comprising a single top foil against a rotating disc. It was noted that Inconel X-750 top foil and a PS304-coated runner disc provide the best low-speed frictional performance. The authors also showed that the roughest counter-face surfaces (Korolon™ 1350A coated foil and PS304-coated runner disc) provided the lowest speed hydrodynamic lift-off and hydrodynamic friction. Korolon™ 1350A is a 25-μm-thick nickel-chromium coating with an overcoat of 50-μm-thick WS_2 including solid lubricants. The resulting surfaces from the reported tests are shown in Fig. 8.

Heshmat et al. [57] reported a breakthrough in the performance of foil thrust bearings in terms of load-carrying capacity, speed, and operating temperature through the use of Korolon™ 1350A coating, which allowed for bearing operation at temperatures of up to 815 °C with PS304 as a composite solid lubricant. PS304 contains silver (10% wt), eutectic barium fluoride (5% wt), and calcium fluoride (5% wt) combined with a chromium oxide hardener (20% wt) within a nickel-chromium matrix (60% wt). While silver is used for low-temperature solid lubrication, eutectic barium and calcium fluoride are used as solid lubricants operating from ambient to 900 °C. The nickel chromium-to-chromium oxide ratio of three to one provides a comparable thermal expansion coefficient (12.4×10^{-6} m/°C) to that of common substrate materials such as Inconel X-750 (14×10^{-6} m/°C) [72]. Low-temperature lubricating characteristics of silver complement the high-temperature characteristics of the eutectic barium fluoride and calcium fluoride to provide self-lubrication from ambient to 900 °C [73]. Dykas and Tellier [31] also chose a PS304-coated runner against an Inconel X750 top foil to investigate early component life wear and reported similar findings.

Fanning and Blanchet [10] noted that HVOF-deposited PS304 disc coatings (using a hydrogen-fueled system) provided enhanced lift-off and touch-down speeds. It also required fewer running-in cycles to reach steady-state conditions.

Blanchet et al. [73] investigated the use of PS304 in thrust-washer tests, running against Inconel X-750 at low contact pressures of 40 kPa, sliding speeds of 5.4 m/s and both ambient and 500°C temperatures to simulate conditions in air foil bearings during startup/shutdown conditions. In all cases, the coefficient of friction was around 0.5, while the wear-rate ranged from 1 to 3×10^{-4} mm^3/Nm. They noted that running under continuous sliding resulted in the roughening of surfaces ($R_q > 2\ \mu$m) and large recesses with (>100 μm) were filled with fine debris, observed on the wear track. This was in contrast with the observation of surface polishing (smoothening) high-temperature foil-bearing operations experienced in cyclic startup and shutdowns.

According to Heshmat et al. [50], running of PS304 against Inconel X750 foils at elevated temperatures, upward of 650 °C, in start–stop cycles led to target roughness of $R_q = 0.1\ \mu$m, but the

generated glossy surface was achieved after consuming many foil bearings. Furthermore, the load-carrying capacity when the same foil was used against PS304 was around 10% of the case where a thin dense chromium coating was applied on the runner surface. The results of tests carried out by Radil and DellaCorte [74] confirm that without the presence of such low-friction glossy surfaces, high starting torques and reduced load-carrying capacities are inevitable.

5 Performance Evaluation of Coatings on Foil Thrust and Journal Bearings

A summary of key coatings presented in the preceding sections is provided in Tables 1 and 2 of the Appendix, for foil journal and thrust bearings, respectively. In low-temperature applications, the use of soft coatings such as MoS_2 and polymer composite coatings has been effective. These coatings are generally limited to relatively low thermal conductivities and diffusivity, high thermal expansion coefficients, and limited maximum operation temperatures. However, it must be noted that the specific properties can vary depending on the exact composition and structure of coating. These coatings are commonly applied to the foil as at high Peclet numbers (Pe), resulting from appreciable sliding speeds before lift-off or shutdown, the contact temperature rise is controlled primarily by the journal and rotor coating thermal properties as shown in Eq. (7). The low-friction soft coatings help to minimize the generated heat in the contact (Eq. (5)). These coatings are paired with conductive journal and rotor coatings such as nickel-chromium or Cr_2O_3 based coatings.

At higher temperatures, hard wear-resistant ceramic coatings and metal matrix composites are more commonplace. The oxidation resistance of these coatings allows for higher upper operating temperatures experienced in these applications. To maintain low abrasive wear high surface hardness of the two surfaces is key. Coatings such as nickel-chromium also can minimize differences in thermal expansion coefficients of coating and substrate (depending on the substrate material's thermal properties) (Eq. (8)) while high thermal conductivity reduces temperature differences between the coating and substrate (Eqs. (7) and (9)). To minimize frictional heat generation (Eq. (5)), composite coatings are used such as PS400, containing friction-mitigating silver, eutectic barium fluoride, and calcium fluoride.

When coatings such as hydrogenated DLCs are used, considerations of the thermal implications are key, among other important properties. For example, the foil-on-disc test rig used by Jahanmir et al. [9] showed the importance of rotor coating thermal properties. Jahanmir et al. [9] investigated the difference in the performance of DLC and chromium-coated rotors. At higher temperatures, the DLC-coated rotor led to accelerated wear of the WS_2-coated foils. This in part is due to the rise in interfacial temperature in the contact caused by the thermal conductivity of the rotor DLC coating (Eq. (7)). The nascent gas film formed during lift-off can also be reduced due to elevated gas film temperatures and interfacial slip (Eq. (2)).

At a high-performance level, air foil bearings incorporating smart materials have been proposed by Martowicz et al. [75]. The implication for thermal monitoring and structural and thermal control, integrated into coating design, is quite promising. Designing the tribological coating system, thermal management system, and machine operating performance together through advance monitoring techniques provides a promising route to advanced machine performance. There is however a significant demand from emerging industries for high volume lower cost air foil bearings requiring advancements in low-cost mass production manufacturing for air foil-bearing coatings and this poses a significant challenge.

6 Concluding Remarks

The effective performance of air foil bearings in high-speed applications relies heavily on advanced coatings for both journal and thrust bearings. The current study emphasizes the crucial role of coatings in overcoming challenges during startup, shutdown, and high-temperature operations. It categorizes coating technologies according to temperature ranges of applications, highlighting specific composite coatings, for breakthrough improvements in load-carrying capacity and reduction of friction. The insights provided offer a roadmap for enhancing the efficiency and reliability of air foil bearings in various industrial applications, particularly in turbomachinery.

Conflict of Interest

There are no conflicts of interest.

Data Availability Statement

No data, models, or code were generated or used for this article.

Nomenclature

c = empirical wear constant
d = thickness of coating
h = film thickness
m = work hardening exponent
p = pressure
q = coulombic frictional heat
A = apparent interfacial contact area
D = depth of heat penetration
H = hardness
K = thermal conductivity
L = contact length
N = contact load
T = temperature
W = wear volume
h_m = minimum film thickness
k_b = Boltzmann's constant
k_o = wear coefficient
q_2 = heat transferred to the foil
E_c = Young's modulus of elasticity
K_{Ic} = plane strain fracture toughness
R_e = effective radius
T_f = friction torque
T_m = maximum flash temperature rise
E' = composite (effective) modulus of elasticity
Kn = Knudsen number
Pe = Peclet number
ΔT = temperature difference between coating and substrate

Greek Symbols

α = coefficient of thermal expansion
β = average asperity tip contact radius
γ = frictional heat partition ratio
δ = molecular diameter
$\Delta\sigma_T$ = change in thermally induced interfacial stress
κ = thermal diffusivity
λ = Stribeck gas film ratio
μ = coefficient of boundary friction
ν_c = Poisson's ratio of coatings
σ = root mean square surface roughness
σ_y = yield stress
τ = ratio of coated and uncoated flash temperature rise
Ψ = plasticity index
ω = angular velocity

Appendix

Tables 1 and 2

Table 1 Foil journal bearing coatings

Paper	Foil coatings investigated	Journal material/coating	Test equipment	Test conditions	Comments	Coating ranking/recommendation
Bagiński and Żywica [56]	• AS20(PTFE) • TiAlN (titanium aluminum nitride) • WC/C (tungsten carbide) • MoS_2/C (carbon-doped molybdenum disulfide) • TiAlN + MoS_2/C	Chromium oxide Cr_2O_3	Foil-bearing test rig	• 30–40 °C • 120 s, startup • Ramp up to 24,000 rpm • Shutdown • Varying loads	• Foil material: Inconel 718 • Max temperature of AS20 and WC/C of 300 °C all the others are >500 °C • Concern about particulate from solid lubricant MoS_2	• MoS_2/C best friction, wear unacceptable • TiAlN low wear but high friction • TiAlN + MoS_2/C low friction and wear
Zywica et al. [5]	AS20(PTFE)	Chromium oxide Cr_2O_3	Foil-bearing test rig	10,000 start/stop cycles at room temperature		N/A
DellaCorte and Edmonds [65]	Inconel X750 (foil and pin for pin on disc)	• PS304 (Ni-Cr binder matrix, chrome oxide hardener and Ag and fluoride solid lubricants) • PS400 (NiMoAl binder matrix, see above for rest)	Foil bearing on Capstone Oil-Free 30 kW microturbine engine and pin on disc	3000 cycles and 10,000 h on engine at 540 °C	• PS400 has better friction than PS304 at room temperature and better high temperature friction and wear • Initial high temperature work required to create lubricious glaze	Inconel X750 foil and PS400-coated journal
Heshmat et al. [50]	• Korolon™ 700 (50 μm polymer-based coating with solid lubricant) • Korolon™ 800 (50 μm WS_2 with solid lubricants) • Korolon™ 1350A (25 μm nickel-chrome) with an overcoat of Korolon™ 800 (25 μm) • Korolon™ 1350B (5 μm)	• PS304 plasma sprayed (<120 μm) • Hard chrome (<180 μm) • Dense chrome (5 μm) • Korolon™ 1350B (5 μm)	High-speed, high-temperature pad on disc tribometer	• 30–810 °C • Startup • Ramp up to 10,000 rpm • Shutdown • 500 × 100 s cycles	• Foil material Inconel X-750 • Disc (journal) Inconel 718 • Recommended combination shown to work in thrust turbojet	Recommended combination • Top foil: Korolon™ 1350A With an overcoat of Korolon™ 800 • Journal: dense chrome coating
Radil and DellaCorte [74]	• Soft polymer (polyimide) • Ceramic (alumina) nickel-based superalloy	PS304 (plasma-sprayed solid lubricant: 10% Ag and 10% BaF_2 and CaF_2, 20% Cr_2O_3 and 60% Ni-Cr binder)	Foil-bearing test rig	• Load increments at 30,000 rpm	• Coatings with solid lubricant properties increase load capacity during boundary and mixed lubrication conditions • When using PS304-coated shafts, high-temp start–stops produce smooth oxide layers. Conforming surfaces and transfer films on the foil	Soft polymer (polyimide)
DellaCorte [76]	Precipitation-hardened Ni-Cr alloy, Inconel X-750, 0.10 mm thick	Super alloy coated with PS304 (modified chrome oxide: 60% wt, Ni-Cr binder, 20% wt Cr_2O_3 hardener, and 10% wt each Ag and BaF_2 CaF_2 lubricants)	Partial arc foil bearing test rig	• 25–650 °C • 20 s startup/shutdown cycle • Ramp up to 13,800 rpm • 30,000 cycles	• Coating is plasma sprayed • Transfer film is important for wear reduction • Wear higher at 25 °C	PS304 shown to be promising

Table 1 *Continued*

Paper	Foil coatings investigated	Journal material/coating	Test equipment	Test conditions	Comments	Coating ranking/recommendation
Bhushan et al. [7]	CdO-graphite-AG (8–10 μm) Cr_2O_3 (sputtered 1 μm)	Ni-Cr-bonded Cr3C2 (detonation gun and ground—60–90 μm)	Full bearing test rig	• 427–650 °C • Start–stop cycles • Shock loading at 30,000 rpm	• Both preferred coating combinations survive 900 start–stop cycles at various loads and temperature • Both coating systems survived shock testing	Foil coatings with CdO-graphite-AG (8–10 μm) and Cr_2O_3 (sputtered 1 μm) Worked well with journals coated with Ni-Cr-bonded Cr3C2 (detonation gun and ground—60–90 μm). Up to 427 °C and 650 °C, respectively
Bhushan and Gray [35]	TiC (sputtered) Cr_2O_3 (sputtered) Cr_2O_3 (chemically adhered) CdO-graphite Uncoated Si_3N_4	Cr_2O_3 (chemically adhered) Cr_2O_3 (sputtered) Tribaloy 800 NASA PS-106 (plasma sprayed) NASA PS-120	Full bearing test rig	• Start–stop test cycles for screening both at room temperature and 650 °C	• Best combinations completed 1000 cycles at 650 °C and 1000 cycles at room temperature. At 14 kPa load • Cr_2O_3 against itself also completed 2000 cycles at 35 kPa	• Foil with air-sprayed CdO-graphite (8–10 μm) against a Ni-Cr-bonded Cr_3C_2 (60–90 μm). Max temperature 370 °C • Uncoated heat-treated foil against NASA PS120 with Ni-aluminide undercoat (140–165 μm). Max temperature 540 °C • Chemically adherent Cr_2O_3 (1.3–2.5 μm against itself (8–13 μm). Max temperature 650 °C
Bhushan [60]	Cr_2O_3 Cr_2O_3 with metallic binder (Ni-Cr)	Cr_3C_2	Partial bearing and full bearing test rig	• Partial bearing and full bearing test rig	• It was found that sputtered chrome oxide is effective at preventing damage up to 650 °C • Protective oxides are formed on the chrome oxide film above 650 °C	Cr_2O_3 with Cr_3C_2 completed 3000 cycles at 650 °C in the partial bearing rig and 9000 cycles at 450 °C in the full bearing test rig. It also survived 3000 start–stop cycles at 35 kPa and 100 g of impact at 30,000 rpm
Bhushan [61]	CdO-graphite CdO-graphite-Ag	Cr_3C_2	Full foil air bearing	• Start–stop test conducted at 14 kPa, 288 °C, and 35 kPa, 427 °C • Oven tests	• Wear performance at 288 °C, 14 kPa CdO-graphite against preoxidized foil and CdO-graphite foil and Cr_3C_2 journal are the same • CdO-graphite on the foil and journal significantly improved hear life at 288 °C but not at 427 °C • CdO-graphite-Ag performs much better than CdO-graphite at 427 °C	CdO-graphite-Ag with Cr_3C_2

Table 1 *Continued*

Paper	Foil coatings investigated	Journal material/coating	Test equipment	Test conditions	Comments	Coating ranking/recommendation
Bhushan and Gupta [39]	• Cr_2O_3 (1 μm) • 75%Cr_2O_3 (1 μm), 25% nichrome top layer, 75% Cr_2O_3 • 75%Cr_2O_3 (0.6 μm), 25% nichrome • Top layer 75%Cr_2O_3, 25% nichrome (0.7 μm), interlayer nichrome coating (0.3 μm)	Nichrome-bonded chrome carbide (75% Cr_3C_2 and 25% nichrome) was applied with a detonation gun on A-286 journal 175–200 μm thick and was ground to a thickness of 62–88 μm with a surface roughness 0.04–0.05 centre line average	Partial pad and full air foil bearing	• Static oven test • Start–stop test • Impact test • Room temperature to 650 °C	• Successfully completed 3000 cycles each at 650 °C, normal load of 14 kPa in the partial arc bearing tests • Successful full bearing tests • 9000 start–stop cycles at a maximum test temperature of 427 °C • Start–stop cycles at a higher normal load of 35 kPa. The coatings were able to survive for 3000 start–stop cycles • The coatings survived 100 g impact with the journal running at 30,000 rpm	Chrome oxide coating sputtered onto InconelX-750 foil, against a detonation gun applied chrome carbide on the A286 journal
Stanford and DellaCorte [66]	• Cu-4Al (ion diffusion) on Inconel X-750 • Inconel X-750 uncoated	PS304	Generation 1 foil air bearing	• 4000 rpm • 25 and 650 °C • 10.3 kPa	• 30,000 start–stop cycles completed	Cu-4Al prevents wear at high temperature Although can cause higher wear at room temperature
Suriano [77]	• Kaman DES (chemically adherent chrome oxide) • Kaman DES + Au • Co-20Ni (electroplated) • TiC	Kaman SCA-coated journal (Cr_2O_3 containing Al_2O_3, SiO_2, and Cr_2O_3)	Foil-bearing test rig	650 °C	• Kaman SCA/TiC best excellent for low break away friction and wear • Kaman SCA and DES are compatible but thicker DES coatings to be investigated for better foil wear characteristics	Kaman SCA/TiC is best outcome

Table 2 Foil thrust bearing coatings

Paper	Foil coatings investigated	Countersurface	Test equipment	Test conditions	Comments	Coating ranking/recommendation
Kim et al. [67]	PTFE top foil 50 μm on Inconel X750	Unspecified	Bearing test rig	• 500 N • 12,000–18,000 rpm • 20,000 rpm	Some wear was evident	N/A
Walker et al. [69]	• MoS_2 (10–16 μm) • WS_2 (30 μm) • Ni-P and Si-O (7–8 μm) • Ni-P and Si-O (13–23 μm) • Nitride surface treatment • PS400 (380–500 μm) • Teflon (20–22 μm)	Dimond stylus	Scratch test and oven	ASTM Standards (G171, C1624, and D7187) for scratch test	• Teflon performed poorly before and after environmental exposure • Standard deviation of MoS_2 roughness is much higher than WS_2 after high-temperature exposure	• Ni-P and Si-O (13–23 μm) • MoS_2 • WS_2 • PS400 • All recommended for further testing
Balducchi et al. [68]	Inconel X750 coated with PTFE	Hard-coated titan	Thrust bearing test rig	• Take off and startup toque tests • Up to 35,000 rpm • 60N		N/A
Jahanmir et al. [8]	Tungsten disulfide based (Korolon™ 900)	• Chrome • DLC • H-DLC	High-speed, high-temperature pad on disc tribometer	• 30–500 °C • Startup • Ramp up to 10,000 rpm • Shutdown • 500 × 100 s cycles	• Chrome, DLC, H-DLC all acceptable at room temperature • H-DLC does not provide hydrodynamic lift at higher temperature	Tungsten disulfide-based foil coating Korolon™ 900 with the chrome-plated discs suitable from room temperature to 500 °C
Jahanmir et al. [9]	Korolon™ 900 (50 μm) tungsten disulfide based	• Korolon™ 900 (50 μm) • Cr • H-DLC	High-speed, high-temperature pad on disc tribometer	• Room temperature • Startup • Ramp up to 10,000 rpm • Shutdown • 500 × 100 s cycles	• Room temperature only • Performance is improved when the solid lubricant (e.g., tungsten disulfide-based coating) is on the foil pad and the hard coating (chrome or H-DLC) is on the disk	Tungsten disulfide-based coating (Korolon™900) on the foil pad with either chrome-plated or H-DLC-coated disks
Dykas et al. [31]	Inconel X750	PS304	Thrust bearing test rig	• Start–stop tests • 425 °C • 7–70 kPa • 23,000 rpm • 1000 cycles	Some wear evident	N/A
Fanning and Blanchet [10]	• Korolon™ 1350A (50 μm thickness, 3 μm Rq nickel-chrome) • Inconel X750 (uncoated, 0.13 μm Rq)	• PS304 plasma-sprayed (0.25 mm thickness, 0.63 μm Rq) • PS304 HVOF-deposited (0.29 μm Rq mm) • Inconel 718 (uncoated, 0.13 μm Rq) PS304-coated discs were heat-treated at 650 °C in air for 25 h to increase coating strength then their surfaces were reground	Thrust runner disc against single thrust top foil	• 540 °C • 250 cycles • 0–5000 rpm (19 m/s) ramp up (8 s), 5000 rpm (10 s) and down to 0 rpm (75 s)	When the top foil was coated with: K1350A hydrodynamic performance improved (reduced lift-off and touch-down speeds)	• Korolon™ 1350A/PS304 hydrodynamic lift of and friction performance (roughest combination) • Inconel X750/PS304 best low-speed friction

Table 2 *Continued*

Paper	Foil coatings investigated	Countersurface	Test equipment	Test conditions	Comments	Coating ranking/recommendation
Heshmat et al. [57]	• Korolon™ 700 (50 μm polymer-based coating with solid lubricant) • Korolon™ 800 (50 μm WS_2 with solid lubricants) • Korolon™ 1350A (25 μm nickel-chrome) with an overcoat of Korolon™800 (25 μm) • Korolon™ 1350B (5 μm)	• PS304 plasma sprayed (<120 μm) • Hard chrome (<180 μm) • Dense chrome (5 μm) • Korolon™ 1350B (5 μm)	High-speed, high-temperature pad on disc tribometer	• 30–810 °C • Startup • Ramp up to 10,000 rpm • shutdown • 500 × 100 s cycles	• Foil material Inconel X-750 • Disc (journal) Inconel 718 • Recommended combination shown to work in thrust turbojet	Recommended combination: • Top foil: Korolon™ 1350A With an overcoat of Korolon™ 800 • Journal/runner: dense chrome coating
Licht [20]	MoS_2 5 μm-coated top foil	Cr_2O_3-coated runner	Air-bearing rig	• Up to 24,000 rpm • High pitching imbalances	Acceptable performance once guide pin alignment was ensured increasing radial clearance of antirotation pins	N/A

References

[1] Samanta, P., Murmu, N. C., and Khonsari, M. M., 2019, "The Evolution of Foil Bearing Technology," Tribol. Int., **135**, pp. 305–323.
[2] Hou, Y., Zhao, Q., Guo, Y., Ren, X., Lai, T., and Chen, S., 2021, "Application of Gas Foil Bearings in China," Appl. Sci., **11**(13), p. 6210.
[3] Kumar, J., Khamari, D. S., Behera, S. K., and Sahoo, R. K., 2022, "A Review of Thermohydrodynamic Aspects of Gas Foil Bearings," Proc. IMechE, Part J: J. Eng. Tribol., **236**(7), pp. 1466–1490.
[4] Branagan, M., Griffin, D., Goyne, C., and Untaroiu, A., 2015, "Compliant Gas Foil Bearings and Analysis Tools," ASME. J. Eng. Gas Turbines Power, **138**(5), p. 054001.
[5] Zywica, G., Baginski, P., and Banaszek, S., 2016, "Experimental Studies on Foil Bearing With a Sliding Coating Made of Synthetic Material," ASME J. Tribol., **138**(1), p. 011301.
[6] Bhushan, B., 1980, "High Temperature Self-Lubricating Coatings for Air-Lubricated Foil Bearings for the Automotive Gas-Turbine Engine," NASA, Report No. NASA-CR-159848.
[7] Bhushan, B., Ruscitto, D., and Gray, S., 1978, "Hydrodynamic Air Lubricated Compliant Surface Bearing for an Automotive Gas Turbine Engine. 2: Materials and Coatings," NASA, Report No. NASA-CR-135402.
[8] Jahanmir, S., Heshmat, H., and Heshmat, C., 2009, "Evaluation of DLC Coatings for High-Temperature Foil Bearing Applications," ASME J. Tribol., **131**(1), p. 011301.
[9] Jahanmir, S., Heshmat, H., and Heshmat, C., 2009, "Assessment of Tribological Coatings for Foil Bearing Applications," Tribol. Trans., **52**(2), pp. 231–242.
[10] Fanning, C. E., and Blanchet, T. A., 2008, "High-Temperature Evaluation of Solid Lubricant Coatings in a Foil Thrust Bearing," Wear, **265**(7–8), pp. 1076–1086.
[11] Heshmat, H., Walowit, J. A., and Pinkus, O., 1983, "Analysis of Gas Lubricated Foil Journal Bearings," ASME J. Lubr. Tribol., **105**(4), pp. 647–655.
[12] Su, H., Rahmani, R., and Rahnejat, H., 2016, "Thermohydrodynamics of Bidirectional Groove Dry Gas Seals With Slip Flow," Int. J. Therm. Sci., **110**, pp. 270–284.
[13] Shahdhaar, M. A., Sandeep, S. Y., Debanshu, S. K., and Suraj, K. B., 2020, Numerical Investigation of Slip Flow Phenomenon on Performance Characteristics of Gas Foil Journal Bearing, SN Appl. Sci., **2**, pp. 1–18.
[14] Lee, N. S., Choi, D. H., Lee, Y. B., Kim, T. H., and Kim, C. H., 2002, "The Influence of the Slip Flow on Steady-State Load Capacity, Stiffness and Damping Coefficients of Elastically Supported Gas Foil Bearings," Tribol. Trans., **45**(4), pp. 478–484.
[15] Gohar, R., and Rahnejat, H., 2018, *Fundamentals of Tribology*, 3rd ed., World Scientific, London.
[16] Lehn, A., 2017, "Air Foil Thrust Bearings: A Thermo-Elasto-Hydrodynamic Analysis," PhD Thesis, Technische Universität Darmstadt.
[17] Salehi, M., Swanson, E., and Heshmat, H., 2001, "Thermal Features of Compliant Foil Bearings—Theory and Experiments," ASME J. Tribol., **123**(3), pp. 566–571.
[18] Tian, X., and Kennedy, F. E., 1993, "Temperature Rise at the Sliding Contact Interface for a Coated Semi-Infinite Body," ASME J. Tribol., **115**(1), pp. 1–9.
[19] Kennedy, F. E., and Tian, X., 2016, "Modeling Sliding Contact Temperatures, Including Effects of Surface Roughness and Convection," ASME J. Tribol., **138**(4), p. 042101.
[20] Licht, L., 1978, "Foil Bearings for Axial and Radial Support of High Speed Rotors: Design, Development, and Determination of Operating Characteristics," NASA, Report No. NASA-CR-2940.
[21] LaTray, N., and Kim, D., 2020, "Design of Novel Gas Foil Thrust Bearings and Test Validation in a High-Speed Test rig," ASME J. Tribol., **142**(7), p. 071803.
[22] Zheng, Y., Chen, S., Lai, T., Zhang, X., and Hou, Y., 2016, "Numerical and Experimental Study on the Dynamic Characteristics of the Foil Journal Bearing With Double-Layer Protuberant Support," J. Adv. Mech Des., Syst., Manuf., **10**(2), pp. 1–12.
[23] Zhou, Q., Hou, Y., and Chen, R. G., 2012, "Development of Foil Thrust Bearings With Simple Structure for Micro Turbines," Adv. Mater. Res., **368**, pp. 1392–1395.
[24] Dykas, B., Bruckner, R., DellaCorte, C., Edmonds, B., and Prahl, J., 2008, "Design, Fabrication, and Performance of Foil Gas Thrust Bearings for Microturbomachinery Applications," ASME. J. Eng. Gas Turbines Power, **131**(1), p. 012301.
[25] Supreeth, S., Ravikumar, R. N., Raju, T. N., and Dharshan, K., 2022, "Foil Stiffness Optimization of a Gas Lubricated Thrust Foil Bearing in Enhancing Load Carrying Capability," Mater. Today, **52**, pp. 1479–1487.
[26] Bruckner, R. J., 2004, "Simulation and Modeling of the Hydrodynamic, Thermal, and Structural Behavior of Foil Thrust Bearings," Ph.D. dissertation, Case Western Reserve University, Cleveland, Ohio.
[27] Lee, D., and Kim, D., 2011, "Three-Dimensional Thermohydrodynamic Analyses of Rayleigh Step Air Foil Thrust Bearing With Radially Arranged Bump Foils," Tribol. Trans., **54**(3), pp. 432–448.
[28] Somaya, K., Yoshimoto, S., and Miyatake, M., 2009, "Load Capacity of Aerodynamic Foil Thrust Bearings Supported by Viscoelastic Material," Proc. IMechE, Part J: J. Eng. Tribol., **223**(4), pp. 645–652.
[29] Xu, F., Dong, Z., Chu, J., Wang, H., and Wang, Y., 2022, "Experimental Analysis of Influence of Double-Layer Bump Foils on Aerodynamic Thrust Foil Bearings Performance," Ind. Lubr. Tribol., **74**(1), pp. 127–133.
[30] Tian, X., and Kennedy, F., 1994, "Maximum and Average Flash Temperatures in Sliding Contacts," ASME J. Tribol., **116**(1), pp. 167–174.
[31] Dykas, B. D., and Tellier, D. W., 2008, "A Foil Thrust Bearing Test Rig for Evaluation of High Temperature Performance and Durability," Army Research Laboratory, Report No. ARL-MR-0692.
[32] Holmberg, K., and Matthews, A., 2009, *Coatings Tribology: Properties, Mechanisms, Techniques and Applications in Surface Engineering Tribology and Interface Engineering Series*, Elsevier, Oxford, UK.
[33] Bull, S. J., and Jones, A. A., 1996, "Multilayer Coatings for Improved Performance," Surf. Coat. Technol., **78**(1–3), pp. 173–184.
[34] Teodorescu, M., Rahnejat, H., Gohar, R., and Dowson, D., 2009, "Harmonic Decomposition Analysis of Contact Mechanics of Bonded Layered Elastic Solids," Appl. Math. Model., **33**(1), pp. 467–485.
[35] Bhushan, B., and Gray, S., 1980, "Development of Surface Coatings for Air-Lubricated Compliant Journal Bearings to 650 °C," ASLE Trans., **23**(2), pp. 185–196.
[36] Greenwood, J. A., and Williamson, J. B., 1966, "Contact of Nominally Flat Surfaces," Proc. R. Soc., A, **295**, pp. 300–319.
[37] Archard, J. F., and Hirst, W., 1956, "The Wear of Metals Under Unlubricated Conditions," Proc. R. Soc. A, **236**(1206), pp. 397–410.
[38] Hornbogen, E., 1975, "The Role of Fracture Toughness in the Wear of Metals," Wear, **33**(2), pp. 251–259.
[39] Bhushan, B., and Gupta, B. K., 1991, *Handbook of Tribology: Materials, Coatings, and Surface Treatments*, McGraw Hill, New York, NY.
[40] Bhushan, B., 2013, *Introduction to Tribology*, 2nd ed., Wiley, New York.
[41] Matthews, A., Franklin, S., and Holmberg, K., 2007, "Tribological Coatings: Contact Mechanisms and Selection," J. Phys., D: Appl. Phys., **40**(18), p. 5463–5475.
[42] Erdemir, A., and Hochman, R. F., 1988, "Surface Metallurgical and Tribological Characteristics of TiN-Coated Bearing Steels," Surf. Coat. Technol., **36**(3–4), pp. 755–763.
[43] Johnson, K. L., 1985, *Contact Mechanics*, Cambridge University Press, Cambridge, UK.
[44] Johns-Rahnejat, P. M., and Gohar, R., 1997, "Point Contact Elastohydrodynamic Pressure Distribution and Sub-Surface Stress Field," Tri-Annual Conference on Multi-Body Dynamics: Monitoring and Simulation Techniques, Bradford, UK, March 21, pp. 161–172.
[45] Johns-Rahnejat, P. M., Dolatabadi, N., and Rahnejat, H., 2020, "Analytical Elastostatic Contact Mechanics of Highly-Loaded Contacts of Varying Conformity," Lubricants, **8**(9), p. 89.
[46] Johns-Rahnejat, P. M., Dolatabadi, N., and Rahnejat, H., 2024, "Elastic and Elastoplastic Contact Mechanics of Concentrated Coated Contacts," Lubricants, **12**(5), p. 162.
[47] Lei, J. F., Martin, L. C., and Will, H. A., 1997, "Advances in Thin Film Sensor Technologies for Engine Applications," ASME 1997 International Gas Turbine and Aeroengine Congress and Exhibition, Florida, USA, June 2–5, 1997, Paper No. V004T15A036.
[48] DellaCorte, C., Zaldana, A. R., and Radil, K. C., 2004, "A Systems Approach to the Solid Lubrication of Foil Air Bearings for Oil-Free Turbomachinery," ASME J. Tribol., **126**(1), pp. 200–207.
[49] Wagner, R. C., 1985, "Experimental Test Program for Evaluation of Solid Lubricant Coating as Applied to Compliant Foil Gas Bearings to 315 deg C," NASA, Report No. NASA-CR-174837.
[50] Heshmat, H., Jahanmir, S., and Walton, J. F., 2007, "Coatings for High Temperature Foil Bearings," ASME Turbo Expo: Power for Land, Sea, and Air, Montreal, Canada, May 14–17, vol. 47942, pp. 971–976.
[51] Lubell, D., DellaCorte, C., and Stanford, M., 2006, "Test Evolution and Oil-Free Engine Experience of a High Temperature Foil Air Bearing Coating," ASME Conf. on Turbo Expo: Power for Land, Sea, and Air, Paper No. GT2006-90572.
[52] Kaur, R. G., and Heshmat, H. H., 2001, "Testing of Coatings for Use in Compliant Foil Bearings," STLE/ASME Joint Conf., Orlando, FL, Oct. 2001.
[53] Bhushan, B., 1981, "Friction and Wear Results From Sputter-Deposited Chrome Oxide With and Without Nichrome Metallic Binders and Interlayers," ASME J. Lubr. Tech., **103**(2), pp. 218–227.
[54] DellaCorte, C., 2012, "Oil-Free Shaft Support System Rotor Dynamics: Past, Present and Future Challenges and Opportunities," Mech. Syst. Signal Process, **29**, pp. 67–76.
[55] Żywica, G., Bagiński, P., Roemer, J., Zdziebko, P., Martowicz, A., and Kaczmarczyk, T. Z., 2022, "Experimental Characterization of a Foil Journal Bearing Structure With an Anti-Friction Polymer Coating," Coatings, **12**(9), p. 1252.
[56] Bagiński, P., and Żywica, G., 2022, "Experimental Study of Various Low-Friction Coatings for High-Temperature Gas Foil Bearings Under Cold-Start Conditions," ASME J. Eng. Gas Turbines Power, **144**(8), p. 081007.
[57] Heshmat, H., Hryniewicz, P., Walton Ii, J. F., Willis, J. P., Jahanmir, S., and DellaCorte, C., 2005, "Low-Friction Wear-Resistant Coatings for High-Temperature Foil Bearings," Tribol. Int., **38**(11–12), pp. 1059–1075.
[58] Bhushan, B., and Gray, S., 1978, "Static Evaluation of Surface Coatings for Compliant Gas Bearings in an Oxidizing Atmosphere to 650 °C," Thin Solid Films, **53**(3), pp. 313–331.
[59] Bhushan, B., 1979, "Development of RF-Sputtered Chrome Oxide Coatings for Wear Application," Thin Solid Films, **64**(2), pp. 231–241.
[60] Bhushan, B., 1980, "Characterization of RF Sputter-Deposited Chrome Oxide Films," Thin Solid Films, **73**(2), pp. 255–265.
[61] Bhushan, B., 1982, "Development of CdO-Graphite-Ag Coatings for Gas Bearings to 427 °C," Wear, **75**(2), pp. 333–356.
[62] San Andrés, L., and Jung, W., 2018, "Evaluation of Coated Top Foil Bearings: Dry Friction, Drag Torque, and Dynamic Force Coefficients," ASME Turbo Expo: Power for Land, Sea, and Air, June 2018, Paper No. V07BT34A018.

[63] Bhushan, B., 1981, "Structural and Compositional Characterization of RF Sputter-Deposited Cr_2O_3+NiCr Films," ASME J. Lubr. Technol., **103**(2), pp. 211–217.
[64] Benoy, P. A., and Williams, S., 2002, "Investigation of Thermal Processing on the Properties of PS304: A Solid Lubricant Coating," Glenn Research Center Research, Report No. 20992.
[65] DellaCorte, C., and Edmonds, B. J., 2009, "A New Temperature Solid Lubricant Coating for High Temperature Wear Applications," NASA, Report No. NASA/TM-2009-215678.
[66] Stanford, M. K., and DellaCorte, C., 2004, "Friction and Wear Characteristics of Cu-4Al Foil Bearing Coating at 25 and 650 °C," NASA, Report No. NASA/TM-2004-212972.
[67] Kim, T. H., Park, M., and Lee, T. W., 2017, "Design Optimization of Gas Foil Thrust Bearings for Maximum Load Capacity," ASME J. Tribol., **139**(3), p. 031705.
[68] Balducchi, F., Arghir, M., Gauthier, R., and Renard, E., 2013, "Experimental Analysis of the Start-Up Torque of a Mildly Loaded Foil Thrust Bearing," ASME J. Tribol., **135**(3), p. 031702.
[69] Walker, M., Kruizenga, A. M., Pasch, J. J., and Fleming, D., 2017, "Foil Bearing Coating Behavior in CO_2," Sandia National Lab Research, Report No. SAND-2017-8280R.
[70] Lee, Y. B., Kim, C. H., Kong, H., Han, H. G., Lee, J. K., Jo, J. H., and Lee, B. S., 2009, "Coating Material Having Heat and Abrasion Resistance and Low Friction Characteristics," U.S. Patent No. 7,615,291.
[71] Humphrey, E., Morris, N. J., Rahmani, R., and Rahnejat, H., 2020, "Multiscale Boundary Frictional Performance of Diamond Like Carbon Coatings," Tribol. Int., **149**, p. 105539.
[72] Fellenstein, J. A., DellaCorte, C., Moore, K. D., and Boyes, E., 1997, "High Temperature Brush Seal Tuft Testing of Selected Nickel-Chrome and Cobalt-Chrome Superalloys," 33rd Joint Propulsion Conference and Exhibit, No. E-10796: 2634.
[73] Blanchet, T. A., Kim, J. H., Calabrese, S. J., and Dellacorte, C., 2002, "Thrust-Washer Evaluation of Self-Lubricating PS304 Composite Coatings in High Temperature Sliding Contact," Tribol. Trans., **45**(4), pp. 491–498.
[74] Radil, K. C., and DellaCorte, C., 2002, "The Effect of Journal Roughness and Foil Coatings on the Performance of Heavily Loaded Foil Air Bearings," Tribol. Trans., **45**(2), pp. 199–204.
[75] Martowicz, A., Roemer, J., Kantor, S., Zdziebko, P., Żywica, G., and Bagiński, P., 2021, "Gas Foil Bearing Technology Enhanced With Smart Materials," Appl. Sci., **11**(6), p. 2757.
[76] DellaCorte, C., 2000, "The Evaluation of a Modified Chrome Oxide Based High Temperature Solid Lubricant Coating for Foil Gas Bearings," Tribol. Trans., **43**(2), pp. 257–262.
[77] Suriano, F. J., 1981, "Gas Foil Bearing Development Program," Aero Propulsion Laboratory, Air Force Wright Aeronautical Laboratories, Air Force Systems Command, United States Air Force, Report No. AD-A116 692.